

AperTO - Archivio Istituzionale Open Access dell'Università di Torino

Early stages of soil development on serpentinite: the proglacial area of the Verra Grande Glacier, Western Italian Alps

This is the author's manuscript

Original Citation:

Availability:

This version is available <http://hdl.handle.net/2318/154486> since 2020-04-01T23:02:07Z

Published version:

DOI:10.1007/s11368-014-0893-5

Terms of use:

Open Access

Anyone can freely access the full text of works made available as "Open Access". Works made available under a Creative Commons license can be used according to the terms and conditions of said license. Use of all other works requires consent of the right holder (author or publisher) if not exempted from copyright protection by the applicable law.

(Article begins on next page)



UNIVERSITÀ DEGLI STUDI DI TORINO

This is an author version of the contribution:

***Early stages of soil development on serpentinite: the proglacial area of the
Verra Grande Glacier, Western Italian Alps***

published on:

Journal of Soils and Sediments, 2014, DOI: 10.1007/s11368-014-0893-5

The final version is available at:

The final publication is available at Springer via [http://dx.doi.org/10.1007/s11368-014-0893-](http://dx.doi.org/10.1007/s11368-014-0893-5)

15 SOIL FORMATION AND WEATHERING IN TIME AND SPACE

16
17 **Early stages of soil development on serpentinite: the proglacial area of the Verra**
18 **Grande Glacier, Western Italian Alps**

19
20 **Michele E. D’Amico • Michele Freppaz • Giovanni Leonelli • Eleonora Bonifacio •**
21 **Ermanno Zanini**

22
23 M. E. D’Amico (✉) • M. Freppaz • E. Zanini

24 DISAFA and NatRisk, Università degli Studi di Torino, Via Leonardo da Vinci 44, Grugliasco (TO),
25 Italy

26 e-mail: ecomike77@gmail.com

27
28 G. Leonelli

29 Earth Science Department, Università degli Studi di Milano, Via Mangiagalli 34, Milano (MI), Italy

30
31 E. Bonifacio

32 DISAFA, Università degli Studi di Torino, Via Leonardo da Vinci 44, Grugliasco (TO), Italy

33
34
35 (✉) **Corresponding author:**

36 Michele E. D’Amico

37 Tel: +39 3490611313

38 e-mail: ecomike77@gmail.com

Abstract

Purpose: Climate change is driving strong variations in mountain habitats, such as glacier retreat, which is releasing large surfaces soon colonized by vegetation and attacked by weathering and pedogenesis. Many proglacial soil chronosequences have been studied in different parts of the world, but no study is available on early soil development and pedogenesis on serpentinite.

Materials and methods: We analyzed the development of the main chemical (pH, organic matter, nutrients and exchangeable cations) and morphological properties in three soil chronosequences in the Verra Grande Glacier forefield (Italian side of the Monte Rosa Group, Western Alps), characterized by slightly different parent materials (pure serpentinite or serpentinite with small gneiss inclusions) and topography (steep lateral moraines or flat basal till).

Results and discussion: Organic matter accumulation, acidification and base and metal leaching are the most important pedogenetic processes active during early stages of soil formation on serpentinite in the upper subalpine altitudinal belt. These processes are associated with minor changes in color and structure showing weak mineral weathering. Biocycling of nutrients is limited on pure serpentinite because of weak primary productivity of the plant community. Pedogenesis is quite slow throughout the forefield, and it is slowest on pure serpentinite. On flat surfaces, where slow erosion permits a fast colonization by Ericaceae, the podzolization process begins after few centuries since moraine deposition, while on steep slopes more time is required.

Conclusions: Pedogenesis on serpentinite is extremely slow. The fast colonization by grassland species increases the speed of pedogenetic trends where serpentinitic till is enriched by small quantities of P-rich gneiss. The encroachment of forest-shrub species increases the speed of pedogenetic trends thanks to a strong nutrient biocycling.

Keywords Chronofunctions • Italian Alps • Podzolization • Proglacial soil chronosequence • Soil formation • Subalpine soils

69 **1 Introduction**

70 Climate change is driving strong variations in high mountain temperature-limited
71 environments, involving both physical and biological components of the ecosystems. One of
72 the most visible effect is the glacier retreat, which continued with only few interruptions since
73 the end of the Little Ice Age (LIA), around mid 19th century, when glaciers reached their
74 maximum Holocene expansion (Ivy-Ochs et al. 2009).

75 The released surfaces in the proglacial areas (also called "glacier forefields") offer the
76 opportunity of observing the development of soil properties and ecosystem dynamics: habitats
77 characterized by different ages coexist over short distances, reducing the effect of other
78 geographical and climatic factors.

79 The parent material of soils has a prominent importance in the determination of pedogenic
80 trends, especially during the early stages of soil formation. Most of the proglacial
81 chronosequences in the European Alps have been described on sialic substrata, a few on
82 calcareous rocks (e.g. Bernasconi et al. 2011; Egli et al. 2001; Mavris et al. 2010; Dümig et
83 al. 2011; Righi et al. 1999); a similar situation is observed in studies performed in other
84 regions (e.g. Ugolini 1966; Burt and Alexander 1996). Extremely scattered data are available
85 about early soil formation and soil chronosequences on serpentinite (examples of revegetation
86 of drastically disturbed serpentine soils are shown by O'Dell and Claassen 2009), and no
87 proglacial chronosequence has ever been studied on ultramafic substrates.

88 This lack of information exists despite the many specific characteristics of serpentine
89 ecosystems. In fact, even if serpentine habitats represent only less than 1% of the world
90 surface, they are common in most orogenic belts, where they create peculiar habitats
91 characterized by three common traits (Whittaker 1954): sparse plant cover and low primary
92 productivity, high levels of endemisms, and different plant communities compared with
93 neighboring areas. These features are caused by the pedogenetic trends on serpentinite, which
94 lead to the formation of soils (commonly called "serpentine soils") typically characterized by
95 unique chemical and physical properties which reduce plant productivity and create stress and
96 toxicity to non-adapted species (the so called "serpentine syndrome", Jenny 1980; Alexander
97 et al. 2007). The "serpentine syndrome" is often associated with several chemical and
98 physical edaphic factors, such as a low Ca:Mg ratio caused by the high amounts of Mg
99 released from the parent material and abundant heavy metals (Ni, Cr, Co). In addition, soils
100 often have low macronutrient (N, P, K) concentrations both because of their paucity in the
101 parent material and of the low plant productivity and are prone to drought and erosion

processes (Brooks 1987). Bioaccumulation of Ca and nutrients in the organic matter-rich surface horizons, preventing losses of deficient nutrients, associated with strong Mg leaching in acidic soils, are important processes that reduce the typical infertility of "serpentine soils" in the Alps (D'Amico and Previtali 2012; Bonifacio et al. 2013; D'Amico et al. 2014b).

The observation of early development of soil properties and the evaluation of pedogenic processes could give important insights in understanding the factors influencing the specific harsh edaphic properties of serpentine habitats. In particular, the intense weathering processes characterizing freshly ground materials in glacier forefield soils release nutrients (P, Fe, K, Ca) from the parent minerals which may thus be present in relatively high amounts even in soils from nutrient-deficient parent minerals (Roberts et al. 1988). The observation of the different rates and quantities of these elements that are released from the parent till and enter the exchange complex in serpentine soils with different, small amounts of silicic inclusions can give important information on the edaphic limitations for the associated plant colonization and primary succession. On serpentinite, weathering releases also potentially toxic elements (such as Ni and/or excessive Mg), which can deeply impact ecosystem development and surface water quality.

In this work we analyzed soils and observed plant colonization along three serpentine chronosequences on the eastern and western lateral moraine systems and on the flat, stable basal till of an Alpine proglacial area, in order to investigate the pedogenic trends and the specific development of the most important edaphic properties in the upper subalpine belt, in the Verra Grande glacier forefield (Italian side of the Monte Rosa Massif). The main aim was to understand the most important processes active during the early stages of pedogenesis on serpentinite in alpine areas. Early pedogenic processes can help in the identification of the edaphic factors involved in the inhibition of plant colonization on raw serpentinitic materials in recently deglaciated areas.

2 Materials and methods

2.1 Study area

The Verra Grande glacier forefield is located in the upper Ayas valley (Aosta Valley, North-Western Italian Alps, Italy, Fig. 1). A precise dating of the Little Ice Age (LIA) Verra Grande moraine system is missing, as few pictures or paintings are available before 1945. However, historical reconstructions have been performed according to similarities in glacier responses with the nearby Lys Glacier (located 5.5 km east of the Verra Grande glacier, with similar

climatic regimes and neighboring accumulation zones), on which more precise dating is available (Vanni 1945, Cerutti 1985; Carnielli 2005). Some of these reconstructions were performed in the early 20th century, only a few decades after the 1860 LIA secondary glacier maximum, considering the opinions of expert eye witnesses (Monterin 1914). According to these works, the LIA maximum advance (around 1820 in the Lys glacier, Strada 1988) left a terminal moraine near the upper portion of the Pian di Verra Inferiore, at an altitude of about 2070 m a.s.l.; a minor advance ended in 1861, when the glacier approached the terminal moraine, leaving a recessional moraine ca. 80 m north of it (Vanni 1945; Cerutti 1985). However, the results of a dendrochronological study performed in five forested 20x20 m quadrates (A to E in Fig. 1b), in order to constrain the dating of the old LIA deposits, indicated a different minimum age of the southernmost terminal moraine. In fact, a tree sampled on the top of this moraine crest, in the vicinities of the A quadrate, germinated around 1550, thus indicating that this morainic arch was deposited before this period. In B (Fig. 1b), on the outer side of the 1860 moraine, the germination year of the oldest specimen was 1887 (determined following the methods described by Leonelli et al. 2011), whereas on the inner side of the crest (C) the germination of the oldest specimen dated 1892. Moving upward, at D and E quadrates, the germination years of the oldest specimens were 1903 and 1946 respectively, in agreement with the glacier retreat phases. In particular, the evidence of old trees growing on the top of the small terminal moraine south of the 1860 one (the formerly presumed 1821 frontal moraine), dating back to about 1550, testifies that the largest LIA advance happened well before the maximum advances of 1821 and 1850-60 that occurred in most of the Alpine glaciers (Orombelli and Mason, 1997).

Monterin (1914), Sacco (1923), Vanni (1945) showed some other phases of glacial retreat from 1861 until 1945. Therefore it is possible to recognize the materials released during the advance around 1920 and the recessional and lateral moraines abandoned during the 1940s. The small moraines deposited by advances recorded after 1945 (particularly during the 1970-1987 time span) have been destroyed by erosion, and freshly abandoned till is not easily reachable. Since the LIA greatest advance, approximately 3 km were left free of ice, while the altitude of the glacier front increased of more than 600 m, reaching an elevation close to 2700 m a.s.l. in year 2012.

The altitude range of the sampled area is limited to 2070-2320 m of elevation: above this altitude, excessive steepness and the consequent erosion inhibit ecosystem and soil development. Present-day natural timberline in the area is around 2400 m a.s.l., and the sampled sites lie in the upper subalpine belt.

The glacial till is composed of serpentinite of antigoritic type, associated with lenses of chlorite-schists, talc-schists and traces of Ca-bearing minerals derived from rodingite inclusions, belonging to the Zermatt – Saas ophiolite (Mattiolo et al. 1951). The eastern lateral moraines are enriched with small amounts (<10% in volume) of granitic-gneissic clasts, derived from Monte Rosa nappe outcrops.

The climate of the Ayas valley is inner-alpine, continental, with low average yearly precipitation. In Champoluc (1450 m a.s.l., 5 km from the study area), the mean precipitation (including snow-water equivalent) is 730 mm y⁻¹, well distributed throughout the year; the average July rainfall is around 60 mm. Higher values are expected in the proglacial area, because of the higher altitude and because the south-north direction of the Ayas valley increases the advection of warm, moist Mediterranean air masses from the south, increasing summer rainfall, while the proximity to the main Alpine divide allows some spillover of precipitation also from the north during strong foehn wind events (Mercalli 2003). Drought stress is possible during some particularly dry summer seasons. The mean annual temperature is between 0 and +2°C (Mercalli 2003).

The vegetation growing in the proglacial area consists of pioneer communities dominated by *Salix* ssp, *Dryas octopetala* L., basophilous grasses and serpentine endemic and Ni-hyperaccumulator species (Vergnano Gambi and Gabbrielli 1981; Vergnano Gambi et al. 1987), with high bare soil on the western lateral moraines and on the basal till, and with well developed grasslands on the eastern lateral moraines. Scattered portions of the LIA proglacial area and the slopes outside the forefield (climax vegetation) are colonized by forests dominated by European larch (*Larix decidua* Mill.), with sparse stone pine (*Pinus cembra* L.), Norway spruce (*Picea abies* Karst.) and birch (*Betula pendula* Roth) specimens. The understory is dominated by *Rhododendron ferrugineum* L., *Juniperus communis* L. and several Ericaceae.

2.2 Soil sampling and analysis

20 sites (soil samples associated with vegetation surveys) were selected along 3 different chronosequences among many other not-sampled observations: 6 sites were on the western lateral morainic crests (W sites), 5 in the eastern ones (E sites), 7 in the flat intramorainic area (C sites, basal till and remnants of frontal/recessional moraines, where soil and ecosystem development could proceed with weaker disturbances) and 2 in pre LIA sites (deposited during the Late Glacial, Younger Dryas, according to Cerutti 1985) (table 1). The E and W sites were characterized by similar steepness. At each site a phytosociological survey was

completed in homogeneous areas of 16 m², visually estimating the percent cover of each species. Field description of site and soil profile characteristics was carried out according to FAO guidelines (2006).

The following data were collected (in brackets, measure unit and acronyms used from now on): altitude, slope steepness (slope, °), aspect (°), surface rockiness (SR, %), bare soil (NS, %), erosion, the cover of Ericaceae and tree cover (Tcov, calculated as percent area on a 100 m² surface). Erosion, SR, NS, herbaceous species and Tcov were determined by visual area estimation. Plant species were identified according to Pignatti (1992).

Soil pits were dug in the middle of each plot, down to the C horizon (parent material) and the soil profile was described to assess soil development and main pedogenic processes. Approximately 1 kg of soil was collected from the genetic horizons (where possible). In the field we were not able to obtain samples for the calculation of bulk densities because of excessive stoniness, the abundant presence of medium and/or large roots and/or the extreme thinness of pedogenic horizons.

The soil samples were air dried, sieved to 2 mm and analyzed according to the USDA methods (Soil Survey Staff 2004). The pH was determined potentiometrically in water extracts (1:2.5 w/w). Exchangeable Ca, Mg, K and Ni were determined after exchange with NH₄-acetate at pH 7.0. The elements were analyzed by Atomic Absorption Spectrophotometry (AAS, Perkin Elmer, Analyst 400, Waltham, MA, USA). The total C and N concentrations were evaluated by dry combustion with an elemental analyser (CE Instruments NA2100, Rodano, Italy). The carbonate content was measured by volumetric analysis of the carbon dioxide liberated by a 6 M HCl solution. The Organic Carbon (TOC) was then calculated as the difference between total C measured by dry combustion and carbonate-C. Available P (P_{olsen}) was determined by extraction with NaHCO₃. In order to detect the spodic properties of the most developed soils, the oxalate and dithionite-extractable fractions of Fe and Al (Fe_{ox}, Al_{ox}, Fe_d) were measured.

In order to obtain a precise mineralogical characterization of the parent material, the coarse sand fraction of C horizons of different terms of the chronosequences was separated by wet sieving, crushed and analyzed by X-ray diffraction as randomly oriented mounts using a Philips PW1710 diffractometer (40kV and 20 mA, graphite monochromator). Scans were made from 5 to 80 °2θ at a speed of 1 °2θ min⁻¹.

Some indices were calculated, to detect the pedogenic trends and to compare the chemical and morphological properties in the solum (C horizons were excluded) or in specific pedogenic horizons with the parent material. The data derived from E1 and W1 were considered as

parent materials for, respectively, the soils on the eastern lateral moraines, and the ones on the western and central till. TOC contents and pH values were used for building indicators of the two main pedogenic process active on young soils in proglacial areas, which are organic matter accumulation (TOCind) and acidification (pHind). Mineralogical weathering and the formation of pedogenic materials were represented using the Buntley-Westin colour index (BWind, Buntley and Westin 1965). Although it cannot substitute detailed mineralogical or geochemical information, the BW index is a synthetic measure of color changes, it can thus be used to represent all processes that induce a change in Hue and/or in Chroma with respect to the gley-colored ultramafic parent material. We selected this index because it was originally developed for Mollisols, and it is thus not as “hematite-oriented” as others (e.g. redness rating by Torrent et al. (1980) in Mediterranean environments), and because of its simple data requirements. The BWind was calculated from moist Munsell colours: increasing points were attributed to hues with increasing redness (e.g. Gley1: 0; 5Y: 1; 7.5YR: 4) which were multiplied by the chroma.

The selected chemical (TOC and pH) and morphological properties (BWind) of each horizon were multiplied by the horizon thickness, and the obtained values were summed to obtain a single index for each solum. The value of pHind for each horizons was calculated as pH difference from the parent material (i.e. E1 and W1). The single profile indices were normalized to a 0-1 scale, by dividing each value by the highest value obtained in the Verra Grande forefield. As we could not measure the soil bulk density, these indicators represent only a qualitative pedogenic trend, as in e.g. Harden et al. (1991).

All numerical analysis were carried out using R 2.15.1 software (R Development Core Team 2000).

The chronofunctions of the pedogenic development indices and of many other edaphic parameters during early stages of pedogenesis were calculated with the *lm* function. Only young sites (0-190 years old) on the eastern and western lateral moraines were used. The best variable transformation was selected according to the significance obtained; usually, the age factor was log-transformed. The chronofunctions should be interpreted in a qualitative way, as the sampling site number was excessively small to obtain statistically significant data. Significant differences in many edaphic parameters between different vegetation types were also checked and displayed as boxplots, using the *multcomp* R package (Hothorn et al. 2008).

3 Results

3.1 Pedogenic trends along the chronosequences

The differences in parent material composition of Eastern and Western moraines were confirmed by mineralogical analyses. The coarse sand fraction of the C horizons was composed almost exclusively of serpentine minerals on the western side, while micas, quartz, amphiboles, alkali feldspars and plagioclases were clearly visible in the soil parent material of the sites on the eastern moraine (Fig. 2). No major mineralogical variations were observed along the LIA chronosequences (not shown).

Only A, AC/CA and C horizons were observed on all LIA lateral moraines and on the basal till deposited between present day and 1860 (Table 2). Most LIA soils were classified as Haplic Regosols (Eutric, Skeletic) (IUSS Working Group 2006). The organic matter accumulated in A horizons was mostly composed of living or dead roots; weak signs of humification were noted in some of the oldest LIA soils, particularly on the eastern lateral moraines (darker colors, granular structure). On stable basal till, a fast acceleration of pedogenesis was observed on surfaces deposited between the largest LIA advance and ca. 1860, with the development of visibly bleached E horizons, characterized by weak laminar structure and strong weathering of stones. Below this eluvial horizon, an incipient Bs had developed (Entic Podzol). Outside the proglacial area, pre-LIA (late glacial) soils were well developed Podzols (Haplic Podzols, IUSS Working Group 2006) on the eastern side of the valley, Haplic Cambisols (Dystric) on the opposite western slope. A weak mineral weathering in surface horizons of young soils was evidenced by slightly more yellow colors than the bluish substrate (table 2). The chronofunctions of B_{Wind} in soils younger than 190 years old (Eq. 1, Fig. 3a) showed a rather slow increase in color development in young soils, which was only slightly faster on the eastern lateral moraines, which was described by the equation:

$$B_{Wind} = -0.050 + 0.019 * \log(age) \quad (p < 0.01, \text{ non significant intercept}) \quad (1)$$

The B_{Wind} calculated in the late glacial Podzol was much higher than the value predicted by the young soils chronofunction.

TOC_{ind}, indicator of TOC accumulation in all pedogenic horizons, increased faster with time in the eastern lateral moraines soils than in the western ones, but the chronofunction calculated on LIA soils was not significant (Fig. 3b). The rate of TOC accumulation on the flat basal till was often higher. In late glacial soils on the western lateral moraines, the TOC_{ind} values slightly positively deviated from the trend found in younger soils, while the difference on the eastern moraines was much larger.

Solum acidification (pHind) proceeded faster in LIA soils on the eastern crests (Fig. 3c, Eqs. (2) and (3)):

$$\text{pHindW} = -0.249 + 0.098 * \log(\text{age}) \quad (p < 0.05, \text{ non significant intercept}) \quad (2)$$

$$\text{pHindE} = -0.455 + 0.187 * \log(\text{age}) \quad (p < 0.05, \text{ non significant intercept}) \quad (3)$$

The pHind calculated in the late glacial Podzol was much lower than the values predicted by the 0-190 years old soils chronofunction, evidencing a steady state reached between 190 and 11500 years ago; a similar trend was found on the western lateral moraines. The faster acidification on the eastern moraines was confirmed also by the three units decrease of pH value in surface horizons from the youngest to pre-LIA sites (Fig. 3d). On the western moraines, the steady state of pH in surface horizons was uncertain, as the chronofunction (Eq. (5)) was not significant.

$$\text{pHE} = 8.84 - 0.44 * \log(\text{age}) \quad (p < 0.01) \quad (4)$$

$$\text{pHw} = 7.67 - 0.17 * \log(\text{age}) \quad (p < 0.1) \quad (5)$$

The trend in solum acidification on the flat basal till with high plant cover was similar to that measured on the eastern lateral moraines (Fig. 3c and 3d).

Podzolization was identified on the oldest LIA member of the basal till (C8), where Fe_{ox}, Fe_d and TOC were already redistributed to the incipient Bs horizons, and in well developed Podzols on the late-glacial till on the eastern lateral moraines (E6, Table 3).

3.2 Soil chemical properties in surface horizons along the chronosequences

Traces of carbonates were found in the young soils in the Verra Grande forefield, probably derived from lenses of oficalcite included in the serpentinite mass (Table 4). They soon disappeared from surface horizons and from the whole profile in the oldest, acidic soils.

TOC was normally well correlated with many exchangeable elements and available nutrients (Table 5). In surface horizons in particular, exchangeable Mg, Ca and K, and available macronutrients (N and P) were strongly positively correlated with TOC, particularly on the western lateral moraines and on the basal till. On the eastern moraines, the relationships were more confused and often not significant.

N concentrations in surface horizons sharply increased in LIA soils, and were highest on the eastern lateral moraines. In pre-LIA (climax) soils, the N concentrations were slightly lower than in younger soils. N below pioneer communities on the basal till was similar to the western lateral moraines, and lower than below forest-shrub communities (Fig. 4a).

The Ca/Mg ratio, important component of the serpentine syndrome, was usually higher than 0.5 (Table 4), and had a general decreasing trend with age (Fig. 4b). This was particularly visible on the eastern moraines, where the decrease followed Eq. (6).

$$\text{Ca/Mg}_E = 1.96 - 0.21 * \log(\text{age}) \quad (p < 0.01) \quad (6)$$

Available P in surface horizons (Fig. 4c) was at least an order of magnitude lower on the western moraines, composed of pure serpentinite, than on the eastern ones, also in initial soils (0.06 vs. 0.72 mg kg⁻¹). On the eastern lateral moraines, available P increased with time according to the chronofunction (Eq. (7)):

$$\text{P}_{\text{olsen}E} = -2.81 + 0.88 * \log(\text{age}) \quad (p < 0.05, \text{non significant intercept}) \quad (7)$$

Extremely low P_{olsen} values were measured also on the basal till, except where a forest cover with ericaceous shrub understory had developed. On same-age, stable sites on the basal till, P_{olsen} concentration under larch/Ericaceae showed a 10 fold increase compared to pioneer communities, and it increased much faster in the upper soil horizons.

Exchangeable Ni increased in surface layers of LIA soils with time, particularly on the western lateral moraines (Fig. 4d); in older soils, Ni had much smaller values. Exchangeable Ni had a weak correlation with organic carbon (Table 5).

3.3 Depth trends in soil chemical parameters and effect of vegetation

The depth trends of many chemical parameters evidenced the rather different speed of pedogenic development in the different morainic environments in the Verra Grande forefield. In particular, the Ca/Mg ratio was usually higher in subsurface than in surface horizons in the western lateral moraines soils (Fig. 5a), in very young soils in general and in weakly podzolised ones. Exchangeable Ni had higher concentration in subsurface horizons than in surface mineral ones under climax and near-climax forest vegetation in stable positions and in the most weathered soils (Table 3, Fig. 5b). The ratio between Ni concentration in subsurface vs. surface horizons under high larch tree cover but low ericaceous shrubs was not higher than

under pioneer or grassland communities (not shown). The ratio between TOC concentration in subsurface vs. surface horizons was significantly higher under climax and quasi-climax forest communities (with high ericaceous cover, Fig. 5c) than under other vegetation types; the same significant difference is shown for the TOC concentration normalized by horizon thickness (not shown). Pioneer communities were also characterized by a significantly smaller pH decrease in surface horizons along the chronosequences (Fig. 5d).

4 Discussions

4.1 Slow pedogenesis on serpentinite

Several pedogenetic processes occur in the Verra Grande forefield, under the mutual influence of vegetation and parent material mineralogy (Fig. 6).

Soils were weakly developed (Regosols, IUSS Working Group 2006) both from the morphological and chemical points of view, up to 190 years of age. In particular, on the western lateral moraines the soils were the least developed of all. The Buntley-Westin color index suggests a very slow Fe release and crystallization, which can be considered a proxy for a slow mineralogical evolution, particularly in the early stages of pedogenesis. The BW index chronofunction (0-190 years old soils) was slightly steeper on the eastern lateral moraines and on the basal till under larch forest with Ericaceae ("climax" vegetation), thanks to a greater solum thickness associated with more productive and acidifying plant communities. The color development was much greater in the old Podzol on the eastern lateral moraines. The BW index of the old Cambisol in the west was slightly higher than the chronofunction curve, suggesting an increase in the weathering rate in later stages of soil development.

If we compare the soil formation rates in the Verra Grande forefield with the ones calculated in other chronosequences (approximating the bulk density at 1.5 g cm^{-3} as in Egli et al. 2014), we observe particularly slow rates in the western lateral moraine system (Fig. 7a): excluding the coarse fragments, the soil formation rate varied between $0 \text{ t km}^{-2} \text{ y}^{-1}$ in the youngest soils and $432 \text{ t km}^{-2} \text{ y}^{-1}$ in 90 years old soils. Higher rates were calculated in LIA soils on the eastern lateral moraines and on the basal till (highest values in 130 years old soils, up to $1000\text{-}1300 \text{ t km}^{-2} \text{ y}^{-1}$), in the range calculated in other Alpine chronosequences on granitoid rocks (Egli et al. 2014, and calculated from the data shown by D'Amico et al. 2014a). However, in Alpine chronosequences on sialic rocks, the rates were highest in the youngest soils (up to $2600 \text{ t km}^{-2} \text{ y}^{-1}$), and then decreased to $300\text{-}1250 \text{ t km}^{-2} \text{ y}^{-1}$ in older LIA ones, following an exponential decline function, thus confirming a delayed start of pedogenesis on serpentinite-dominated parent materials. A humped curve is expected when relating soil production from

regolith with soil depth (Humphreys and Wilkinson 2007) and similar trends have been observed in post-mining chronosequences on sandy parent materials under boreal forests (e.g. Celi et al. 2013) or in coastal lake sand dunes (Lichter et al. 1998). A greater specificity of the soil parent material seems to be present in proglacial chronosequences as the humped soil formation curve was visible only in serpentine-dominated soils.

The organic matter accumulated in the soil profiles faster in the eastern LIA sites and on the flat basal till, in agreement with the poor primary productivity characterizing the western sites. The accumulation of organic matter in turn influenced the development of all other chemical properties thanks to the increase of the cation exchange capacity that caused a temporary increase in available bases, nutrients and metals.

Another effect mainly related to organic matter accumulation was surface acidification, as frequently reported in proglacial areas (e.g. Bernasconi et al. 2011). The higher organic matter accumulation on the eastern lateral moraines induced a faster pH decrease in surface horizons, while the higher initial carbonate content contributed to the higher intercept of the chronofunction. The trends were similar (slightly higher values on flat surfaces) when considering the acidification of the whole profiles (pH_{ind}). In agreement with the humped curve of the soil formation rate, sigmoid curves could generally represent the variations of soil properties with time. The acidification sigmoid in the Verra Grande chronosequences showed different curve parameters on the different morainic environments: a slow pH decrease characterized the first decades, as shown by the negative intercept of the pH_{ind} chronofunction and the intercept in the surface pH chronofunctions higher than the E1 and W1 values. After the encroachment of vegetation (slower and reduced on the western lateral moraines), the acidification rate increased, to reach a steady state in later stages of soil development (evidenced by the late glacial sites, whose pH and pH_{ind} values lie far from the curve based on LIA sites). On the western lateral moraine, the pH values in 190 years old soils were similar to those characterizing old climax soils, but the high micro-scale variability, shown by the non linearity of the pH decrease on LIA materials, makes the steady state difficult to define. A larger number of samples of intermediate ages might show a better pH trend in this environment.

A sigmoid curve could also properly represent the TOC accumulation and mineral weathering (BW_{ind}) in the western chronosequence, while in the eastern one the speed of soil development increased again in later stages, thanks to the onset of the podzolization process, after some (probably) hundreds or thousands of years.

Comparing the acidification trends on serpentinite and on other substrates from different chronosequences in subalpine environments, we observe a slower and shallower pH decrease on serpentinite, thanks to the base-rich parent material. For example, in the nearby Lys forefield (D'Amico et al. 2014a), the initial pH in freshly deposited gneissic till was 6.6 (ca 1 unit lower than in the western part of the Verra Grande forefield), and it decreased to 4.6 in 130 year old soils. Similar values were obtained in the Damma glacier forefield (Bernasconi et al. 2011). Comparing the TOC concentrations in the most productive chronosequence (eastern lateral moraines), we observe a slower increase, particularly in subsurface horizons, than on gneiss (e.g. D'Amico et al. 2014a; Egli et al. 2001) or in mixed materials (e.g. He and Tang 2008). In order to compare the organic matter accumulation in the Verra Grande chronosequences with other alpine chronosequences, we calculated the TOCind from available data for the Morteratsch (Egli et al. 2012) and Lys forefield (D'Amico et al. 2014). The TOC accumulation in serpentine soils was usually around the lowest limit of the range measured on granitoid rocks (Fig. 7b).

The extremely slow increase in plant cover on pure serpentinite maintained high erosion rates, which reduced the encroachment of new plants and, in turn, slowed down soil development. Erosion was partially reduced by the widespread presence of a thin, black cryptogamic crust, which also increased organic carbon and nutrient concentrations at the surface of these weakly developed soils. Cryptogamic crusts on cold desert soils increase N concentration thanks to N-fixating cyanobacteria and thus ameliorate the physical environment by reducing erosion and increasing water retention; in fact, cryptobiotic crusts are reported to increase the speed of plant colonization (Breen and Levesque 2008). On the essentially flat intramorainic basal till, plant cover increased slightly faster thanks to reduced erosion. However, the species turnover and the chemical variations with time were extremely slow as well (outside the forest patches).

Cryoturbation also limits soil development throughout the Verra Grande forefield, mutually linked with the slow vegetation encroachment and slow pedogenesis. A small active rock glacier, indicator of sporadic permafrost on the Alps (Guglielmin 1997) is present at 2500 m on the western lateral moraine. Evidences of cryoturbation in the soils, such as silt caps on the upper surfaces of stones and a platy vesicular structure, were more visible than in other nearby proglacial areas (D'Amico et al 2014a), possibly thanks to a greater silt content. Frost heave and moving freezing fronts during dry winter months are the main factors involved in silt translocation and the formation of silt caps (Ugolini et al. 2006; Frenot et al. 1995). Frost heave is more effective where vegetation cover is scarce (Ugolini 1966), and its effects

include the formation of platy structure with high porosity (vesicular structure). The establishment of vegetation destroys this cryogenic structure, both because of bioturbation and because of reduction in number and amplitude of freeze-thaw cycles (Crocker and Major 1955; Ugolini 1966).

4.2 The development of serpentine soil properties, and the effect of sialic inclusions

Oficalcite inclusions were probably correlated with the quite high Ca/Mg ratio recorded in young soils of the considered proglacial area, usually higher than 0.5 (Table 3); “normal” values on serpentinite should range between 0.01 and 0.1 (Brooks 1987). Initial soils in the eastern moraine system had the highest Ca/Mg ratio, probably thanks to the presence of plagioclases. The pH decrease may have enhanced carbonate dissolution and Ca leaching, accounting for the decreasing Ca/Mg ratio observed particularly on the eastern lateral moraines. In fact, most acidic soils in Valle d'Aosta have exchangeable Ca/Mg ratios below 1.5, also on sialic parent materials (unpublished data). On serpentinite, under forest vegetation, the lowest values were found in the most acidic podzolic soils, while in other less acidified soils Ca biocycling and bioaccumulation tended to increase the Ca/Mg ratio above unity (D'Amico and Previtali 2012; D'Amico et al. 2014b). The ratio between the Ca/Mg ratio in subsurface vs. surface horizons, however, suggests that actually Ca bioaccumulation occurs only on the eastern moraines and on the basal till (higher values in surface horizons). On the western moraines Ca leaching from surface A horizons, likely associated with the dissolution of carbonate traces, was poorly limited by a weak biocycling associated with the low primary production.

Exchangeable Ni had an initial increase, followed by a decrease in mature soils, with a sharper trend on the western lateral moraines. In the E soils, the initial increase in Ni was small, probably due to the higher acidification rate. Barren soils often have smaller amounts of exchangeable Ni when compared with vegetated sites (Lazarus et al. 2010; Chiarucci 2004); however, in our chronosequences, exchangeable Ni increases faster under low plant cover, while the most developed soils under climax coniferous forest with ericaceous understory have low exchangeable Ni, because of strong leaching (D'Amico and Previtali 2012). The depth trend of exchangeable Ni shows metal leaching from surface and accumulation in deeper horizons below larch forest-ericaceous vegetation also in very young soils, where rejuvenating erosive processes are weak, even if no pedogenic Fe or Al production and leaching were detectable (not shown). This depth trend, dependent on the

abundance of conifers and Ericaceae, could be related to incipient podzolization, initially active on the most mobile metals (such as Ni).

Available phosphorus was probably the single elemental characteristic which differed the most between the two lateral moraine systems. Its concentration rapidly increased on the eastern lateral moraines, after having started at a much higher level on the bare, fresh till, than on the opposite moraine system. In the E sites, the contribution of a sufficient P content, probably derived from the early weathering of sialic rock fragments which contain some P-bearing apatite, permitted a fast, complete colonization by herbaceous species, which reduced erosion despite the slope steepness. It is well known that sialic gneiss and schists (whose presence was verified by XRD analysis) contain 5 or 6 times more P than ultramafic rocks (e.g. Porder and Ramachandran 2013). The more complete plant cover, in turns, is related with the faster increase in TOC concentration in the A horizons on the eastern lateral moraines, accounting for the steeper chronofunction of available P concentration caused by biocycling and bioaccumulation.

On the opposite side of the valley, on pure serpentinite, the P concentration was extremely low throughout the chronosequence, and it was probably one of the most important limiting factors for plant colonization in this area (Nagy and Proctor 1997; Vitousek et al. 2010). Thanks to the good correlation with TOC and, thus, with vegetation productivity, the P concentration had two different trends on the flat basal till; it followed more or less the eastern chronofunction under well developed forest vegetation, while it followed the western chronofunction under pioneer vegetation. A weak P bioaccumulation was induced by the cryptogamic crust on the western moraines, but this was limited to few millimeters on the soil surface. Such decoupling indicates a strong effect of vegetation on the bioaccumulation of available P in surface horizons.

Available P keeps increasing with time and reaches the highest values in the most acidic and the most developed late glacial Podzol, suggesting a different trend with respect to the usual one of E horizons of podzolic soils (Celi et al. 2013). The general trend towards an amelioration of soil fertility was particularly strong under the most productive subalpine forest vegetation. A strong ameliorating effect of conifers on serpentine soils has been recognized during secondary plant successions in many regions of the world, such as Mediterranean Italy (Chiarucci 2004) or the savannahs of eastern USA (Barton and Wallenstein 1997).

4.3 Effect of subalpine vegetation on pedogenesis: incipient podzolization?

Podzols are the climax soils in the subalpine phytoclimatic region, and 600-3000 years are considered necessary for the formation of Podzols on silic materials on the Alps (e.g. Egli et al. 2006; Zech and Wilcke 1977). Much faster rates of Podzol formation have been reported in some proglacial chronosequences in the Aosta Valley, such as in the nearby Lys glacier forefield (D'Amico et al. 2014a): E horizons appeared soon after the establishment of climax subalpine larch forest with a thick ericaceous understory. Also on serpentinite, podzolic soils with thick E horizons overlying weakly developed Bs horizons are commonly found on stable surfaces under subalpine forests with northward aspects in the Aosta Valley (D'Amico et al. 2008), in spite of the fact that the high base content and the fast weathering should inhibit podzolization on ultramafic materials (Lundström et al. 2000). Also in our study area, well developed Podzols were characteristic of late glacial materials, particularly on the slightly colder and less steep eastern side of the valley (profile E6), while on the slightly drier western valley side, only Cambisols (Dystric) were found.

The onset of podzolization seems to have taken place soon after the substitution of pioneer, basophilous plant communities by acidophilous, "climax" ones, on flat surfaces, during the time lapse between the most extensive LIA advance and 1860. Rather high pH values characterize the bleached E horizon in the older LIA podzolic soils. Similarly high pH values were found in surface A and E horizons of podzolized soils on serpentinite (e.g. Sasaki et al. 1968; Lee and Hewitt 1982). We can exclude that this light gray horizon is made of "younger", C-like materials, thanks to the high degree of weathering of the material (the rock fragments were soft and easily crashed by hand pressure), the much lower pH and the widespread presence of this sequence of horizons on the similar-age glacial till.

In the nearby Lys glacier forefield, the largest glacier extent was reached in 1821 (Monterin 1914), and most glaciers in the Alps reached their largest Holocene extension during the first half of the 19th century (Ivy-Ochs et al. 2009). Similarly, the southernmost LIA moraine of the Verra Grande forefield was attributed to the same glacier advance (e.g. Vanni 1945). However, the development degree of the podzolic soils belonging to the largest LIA glacier extension in the Verra Grande forefield seems incompatible with the moraine's young age (from the extremely weakly developed Regosol on the 1861 material to the podzolic soil on the presumed 1821 till). The presumed 1821 materials (between the 1861 recessional and the terminal LIA moraine) could thus be ascribed to older glacier advances. Indeed some glaciers in the Western and Central Alps approached or reached their maximum LIA extent at the end of the 14th or 17th century instead of the 19th century. For example, the Gorner glacier on the

northern flank of the Monte Rosa Massif in Valais (CH) (less than 10 km north of the Verra Grande glacier), reached its maximum LIA extent around 1380 (Holzhauser et al. 2005). Moreover, Mortara et al. (1992), by dating the soil organic fraction in the Ab horizon of two smaller lateral moraines outside the LIA ones (at 2600 m a.s.l. outside the western moraine, and at 2300 m a.s.l. outside the eastern moraine), found that these moraines were deposited at least 950 ± 185 yr B.P. and <200 yr B.P. respectively. The former date witnesses a period of the Holocene before 1820, when the upper part of the Verra Grande Glacier was more extensive than during the LIA peak, whereas the latter evidences the presence of LIA glacial deposits outside the terminal moraine of the LIA maximum. We can also exclude that this glacial material was deposited in more ancient periods (i.e. late glacial), because of the shallowness of the soil profiles, the much weaker weathering degree and the much higher pH values than those of pre-LIA sites. Moreover, it is well known that Alpine glaciers reached their largest Holocene surface during the LIA (Joerin et al. 2006). Although a more precise dating of the southernmost moraine system is necessary for the development of precise chronofunctions for soil and vegetation development, Entic Podzols, with thin albic and weakly developed spodic horizons (C8), seem to form in 500-1000 years in this serpentinite forefield. The time required for Podzol formation on serpentinitic till apparently is some centuries longer than in nearby gneissic till (D'Amico et al. 2014a), but it is still quite short comparing with the normal range necessary for podzol formation on sialic materials in the Alps (Egli et al. 2006; Zech and Wilcke 1977).

5 Conclusions

In this study we evaluated the main pedogenetic processes occurring in recently deglaciated areas on serpentinite in the Western Italian Alps. As usual in proglacial chronosequences, young soils are characterized by acidification, organic matter accumulation and mineral weathering: however, on serpentinite, these processes operate more slowly than on other parent materials. Small quantities of gneiss in the parent till appear to increase the speed of encroachment by grassland species. The higher organic matter input thereby increases the acidification rate and nutrient biocycling. The slopes of the chronofunctions of the main chemical properties and of pedogenetic indicators are often significantly greater and confirm the enhanced rate of pedogenesis where the serpentinitic till is enriched by small quantities of sialic rocks. Strong surface erosion and cryoturbation with very low vegetation cover characterize instead the first few hundreds of years on pure serpentinite. This is associated with soils poor in available nutrients. On flat surfaces (ground moraines), the encroachment

by Ericaceae in particularly stable sites seems associated with the onset of podzolization in few hundreds of years. The strong edaphic limitations to plant encroachment and to primary vegetation succession in young serpentine habitats might make these young ecosystems particularly vulnerable to environmental variations caused by global change.

Acknowledgements This study was performed thanks to the research agreement between the University of Turin, NATRISK centre, and Regione Autonoma Valle d'Aosta, department of soil defense and hydraulic resources. This research was supported by the Italian MIUR Project (PRIN 2010-11; grant number 2010AYKTAB_006): "Response of morphoclimatic system dynamics to global changes and related geomorphological hazards" (national coordinator C. Baroni). The authors wish to thank also the Regione Autonoma Valle d'Aosta office "Assessorato agricoltura e risorse naturali" for the tree sampling permit.

References

- Alexander EB, Coleman RG, Keeler-Wolf T, Harrison SP (2007) Serpentine geoecology of western North America. Oxford University Press, New York
- Barton AM, Wallenstein MD (1997) Effects of invasion of *Pinus virginiana* on soil properties in serpentine barrens in Southwestern Pennsylvania. *J Torrey Bot Soc* 124(4):297-305
- Bernasconi SM, Bauder A, Bourdon A, Brunner I, Bünemann E, Christl I, Derungs N, Edwards P, Farinotti D, Frey B, Frossard E, Furrer G, Gierga M, Göransson H, Gülland K, Hagedorn F, Hajdas I, Hindshaw R, Ivy-Ochs S, Jansa J, Kiczka M, Kretschmar R, Lemarchand E, Luster J, Magnusson J, Mitchell EAD, Venterink HO, Plötze M, Reynolds B, Smittenberg RH, Stähli M, Tamburini F, Tipper ET, Wacker L, Welc M, Wiederhold JG, Zeyer J, Zimmermann S, Zumsteg A (2011) Chemical and biological gradients along the Damma Glacier soil chronosequence, Switzerland. *Vadose Zone J* 10:867-883
- Bonifacio E, Falsone G, Catoni M (2013) Influence of serpentine abundance on the vertical distribution of available elements in soils. *Plant Soil* 368:493-506
- Breen K, Lévesque E (2008) The influence of biological soil crusts on soil characteristics along a High Arctic glacier foreland, Nunavut, Canada. *Arct Antarct Alp Res* 40(2):287–297

639 Brooks RR (1987) Serpentine and its vegetation: a multidisciplinary approach. *Dioscorides*,
640 Oregon

641 Buntley GJ, Westin FC (1965) A comparative study of developmental color in a Chestnut-
642 Chernozem-Brunizem soil climosequence. *Soil Sci Soc Am Proc* 24:128-132

643 Burt R, Alexander EB (1996) Soil development on moraines of Mendenhall Glacier, southeast
644 Alaska. 2. Chemical transformations and soil micromorphology. *Geoderma* 72:19-36

645 Carnielli T (2005) Le variazioni frontali ed areali recenti del Ghiacciaio Grande di Verra
646 (Monte Rosa, Alpi). *Geogr Fis Dinam Quat Suppl* VII: 79-87

647 Celi L, Cerli C, Turner BL, Santoni S, Bonifacio E (2013) Biogeochemical cycling of soil
648 phosphorus during natural revegetation of *Pinus sylvestris* on disused sand quarries in
649 Northwestern Russia. *Plant Soil* 367:122-134

650 Cerutti AV (1985) Le variazioni glaciali e climatiche durante l'ultimo secolo nei gruppi del
651 Monte Bianco e del Monte Rosa. *Geogr Fis Dinam Quat* 8:124-136

652 Chiarucci A (2004) Vegetation ecology and conservation on Tuscan ultramafic soils. *Bot Rev*
653 69:252–268

654 Crocker RL, Major J (1955) Soil development in relation to vegetation and surface age at
655 Glacier Bay, Alaska. *J Ecol* 43(2):427-448

656 D'Amico ME, Previtali F. 2012. Edaphic influences on ophiolitic substrates on vegetation in
657 the Western Italian Alps. *Plant Soil* 351:73-95

658 D'Amico ME, Julitta F, Previtali F, Cantelli D (2008) Podzolization over ophiolitic materials
659 in the western Alps (Natural Park of Mont Avic, Aosta Valley, Italy). *Geoderma*
660 146:129-137

661 D'Amico ME, Freppaz M, Filippa G, Zanini E (2014a) Vegetation influence on soil formation
662 rate in a proglacial chronosequence (Lys Glacier, NW Italian Alps). *Catena* 113:122-137

663 D'Amico ME, Bonifacio E, Zanini E (2014b) Relationships between serpentine soils and
664 vegetation in a xeric inner-Alpine environment. *Plant Soil*, doi: 10.1007/s11104-013-
665 1971-y

666 Dümig A, Smittenberg R, Kögel-Knaber I (2011) Concurrent evolution of organic and
667 mineral components after retreat of the Damma glacier, Switzerland. *Geoderma* 163:83-
668 94

669 Egli M, Fitze P, Mirabella A (2001) Weathering and evolution of soils formed on granitic,
670 glacial deposits: results from chronosequences of Swiss alpine environments. *Catena*
671 45:19-47.

672 Egli M, Wernli M, Kneisel C, Haeberli W (2006) Melting glaciers and soil development in the
 673 proglacial area Morteratsch (Swiss Alps): I. Soil type chronosequences. *Arct Antarct Alp*
 674 *Res* 38(4):499–509.

675 Egli M, Favilli F, Krebs R, Pichler B, Dahms D (2012) Soil organic carbon and nitrogen
 676 accumulation rates in cold and alpine environments over 1Ma. *Geoderma* 183-184:109-
 677 123

678 Egli M, Dahms D, Norton K (2014) Soil formation rates on silicate parent material in alpine
 679 environments: different approaches-different results? *Geoderma* 213:320-333

680 FAO (2006) *Guidelines for Soil Description*. 4th ed. FAO, Rome

681 Frenot Y, Van Vliet-Lanoë B, Gloaguen JC (1995) Particle translocation and initial soil
 682 development on a glacier foreland, Kerguelen Islands, Subantarctic. *Arct Alp Res*
 683 27(2):107-115

684 Guglielmin M (1997) *Il permafrost alpino, concetti morfologia e metodi di individuazione*.
 685 Quaderni di Geodinamica Alpina e Quaternaria, Milano

686 Harden JW (1982) A quantitative index of soil development from field descriptions: examples
 687 from a chronosequence in central California. *Geoderma* 28: 1-28.

688 Harden JW, Taylor EM, Hill C, Mark RK, McFadden LD, Reheis MC, Sowers JM, Wells SG
 689 (1991) Rates of soil development from four soil chronosequences in the Southern Great
 690 Basin. *Quat Res* 35:383-399

691 He L, Tang Y (2008) Soil development along primary succession sequences on moraines of
 692 Hailuoguo Glacier, Gongga Mountain, Sichuan, China. *Catena* 72:259-269

693 Holzhauser H, Magny M, Zumbuhl HJ (2005) Glacier and lake-level variations in west-
 694 central Europe over the last 3500 years. *The Holocene* 15(6):789-801

695 Hothorn T, Bretz F, Westfall P (2008) Simultaneous Inference in General Parametric Models.
 696 *Biometrical J* 50(3):346-363

697 Humphreys GS, Wilkinson MT (2007) The soil production function: a brief history and its
 698 rediscovery. *Geoderma* 139(1-2):73-78

699 IUSS Working Group WRB (2006) *World reference base for soil resources 2006*. World Soil
 700 Resources Reports No. 103. FAO, Rome

701 Ivy-Ochs S, Kerschner H, Maisch M, Christl M, Kubik PW, Schluechter C (2009) Latest
 702 Pleistocene and Holocene glacier variations in the European Alps. *Quat Sci Rev*
 703 28:2137–2149

704 Jenny H (1980) *The Soil Resource: Origin and Behavior*. *Ecol Stud* 37:256–59

705 Joerin UE, Stocker TF, Schlüchter C (2006) Multicentury glacier fluctuations in the Swiss
 706 Alps during the Holocene. *The Holocene* 16 (5):697-704
 707 Lazarus BE, Richards JH, Claassen VP, O'Dell RE, Ferrel MA (2011) Species specific plant-
 708 soil interactions influence plant distribution on serpentine soils. *Plant Soil* 342:327–344
 709 Lee WG, Hewitt AE (1982) Soil changes associated with development of vegetation on an
 710 ultramafic scree, northwest Otago, New Zealand. *J Royal Soc New Zealand* 12(3):229-
 711 242
 712 Leonelli G, Pelfini M, Morra di Cella U, Garabaglia V (2011) Climate warming and the
 713 recent treeline shift in the European Alps : the role of geomorphological factors in high-
 714 altitude sites. *Ambio* 40:264-273
 715 Lichter J (1998) Rates of weathering and chemical depletion in soils across a chronosequence
 716 of Lake Michigan sand dunes. *Geoderma* 85:255-282
 717 Lundström US, van Breemen N, Bain DC (2000) The podzolization process. A review.
 718 *Geoderma* 94:91-107
 719 Mattiolo, E., Novarese, V., Franchi, S., Stella, A., 1951. Carta Geologica d'Italia 1:100000,
 720 foglio 29. Istituto Geografico Militare (Firenze, Italy)
 721 Mavris C, Egli M, Plötze M, Blum JD, Mirabella A, Giaccai D, Haeberli W (2010). Initial
 722 stages of weathering and soil formation in the Morteratsch proglacial area (Upper
 723 Engadine, Switzerland). *Geoderma* 155:359-371
 724 Mercalli L (2003) Atlante climatico della Valle d'Aosta. Società Meteorologica Italiana (Ed),
 725 Torino
 726 Monterin U (1914) Osservazioni sui Ghiacciai del Gruppo del Monte Rosa nel versante
 727 d'Ayas e di Gressoney. *Bollettino del Comitato Glaciologico Italiano* 1:81-103
 728 Mortara G, Orombelli G, Pelfini M, Tellini C (1992) Suoli e suoli sepolti olocenici per la
 729 datazione di eventi geomorfologici in ambiente alpino: alcuni esempi tratti da indagini
 730 preliminari in Val d'Aosta. *Il Quaternario* 5(2):135-146
 731 Nagy L, Proctor J (1997) Plant growth and reproduction on a toxic alpine ultramafic soil:
 732 adaptation to nutrient limitation. *New Phytol* 137:267-274
 733 O'Dell RE, Claassen VP (2009) Serpentine revegetation: a review. *Northeastern Naturalist*
 734 16(Special Issue 5):253–27
 735 Orombelli G, Mason P (1997) Holocene glacier fluctuations in the Italian Alpine region. In:
 736 Frenzel B, Boulton GS, Gläser B, Huckriede (Eds), *Glacier Fluctuations during the*
 737 *Holocene*. *Paläoklimaforschung* 24: 59–65
 738 Pignatti S (1992) *Flora d'Italia*, vol 1–3. Edagricole, Bologna

739 Porder S, Ramachandran S (2013) The phosphorus concentration of common rocks - a
 740 potential driver of ecosystem P status. *Plant Soil* 367:41-55
 741 Righi D, Huber K, Keller C (1999) Clay formation and Podzol development from postglacial
 742 moraines in Switzerland. *Clay Min* 34:319-322
 743 Roberts JA, Daniels WL, Bell JC, Burger JA (1988) Early stages of mine soil genesis in a
 744 Southwestern Virginia spoil lithosequence. *Soil Sci Soc Am J* 52:716-723
 745 Sacco F. (1923). La fronte del Ghiacciaio di Verra (Valle di Ayas) nel 1923. Estratto dal
 746 Bollettino del Comitato Glaciologico Italiano 6
 747 Sasaki S, Matsuno T, Kondo Y (1968) A podsol derived from serpentine rocks in Hokkaido,
 748 Japan. *Soil Sci Plant Nutr* 14:99–109.
 749 Soil Survey Staff (2004) Soil Survey Laboratory Methods Manual, Soil Survey Investigations
 750 Report No. 42
 751 Strada E (1988) Le variazioni del ghiacciaio del Lys dalla “Piccola Glaciazione” ai nostri
 752 giorni. *Natura bresciana, Ann Mus Civ Sc Nat* 24: 275-188
 753 Torrent J, Nettleton WD, Borst G (1980) Genesis of a Typic Durixeralf of Southern
 754 California. *Soil Sci Soc Am J* 44:575-582.
 755 Ugolini FC (1966) Part 3. Soils. In: A. Mirskey (ed) Soil development and ecological
 756 succession in a deglaciated area of Muir Inlet, southeast Alaska. Institute of Polar Studies
 757 report Number 20, Ohio State University, Columbus, Ohio, USA
 758 Ugolini FC, Corti G, Certini G (2006) Pedogenesis in the sorted patterned ground of Devon
 759 Plateau, Devon Island, Nunavut, Canada. *Geoderma* 136:87-106
 760 Vanni M (1945) Il Grande Ghiacciaio di Verra in Valle d’Ayas. Bollettino del Comitato
 761 Glaciologico Italiano e della Commissione Glaciologica del CAI 23:55-86
 762 Vergnano Gambi O, Gabbrielli R (1981) La composizione minerale della vegetazione degli
 763 affioramenti ofiolitici dell’alta Valle d’Ayas. *Rev Valdôtaine Hist Nat* 35:51–61
 764 Vergnano Gambi O, Pedani R, Gabbrielli R (1987) Ulteriori dati sulla composizione minerale
 765 della vegetazione degli affioramenti ofiolitici dell’alta Valle d’Ayas. *Rev Valdôtaine Hist*
 766 *nat* 41:99–110
 767 Vitousek PM, Porder S, Houlton BZ, Chadwick OA (2010) Terrestrial phosphorus limitation:
 768 mechanisms, implications, and nitrogen–phosphorus interactions. *Ecol Appl* 20(1):5–15.
 769 Whittaker RH (1954) The ecology of serpentine soils: a symposium. I. Introduction. *Ecol*
 770 35:258-259
 771 Zech W, Wilcke, BM (1977) Vorlaube ergebnisse einer Bodenchronosequenzstudie im
 772 Zillertal. *Mitteilungen der Deutschen Bodenkundlichen Gesellschaft* 25:571-586

Figure captions

Fig. 1: a) The Verra Grande glacier forefield in the North-western Italian Alps. b) Soil sampling sites (full dots) and forest sites where tree maximum age was detected (full triangles from A to E).

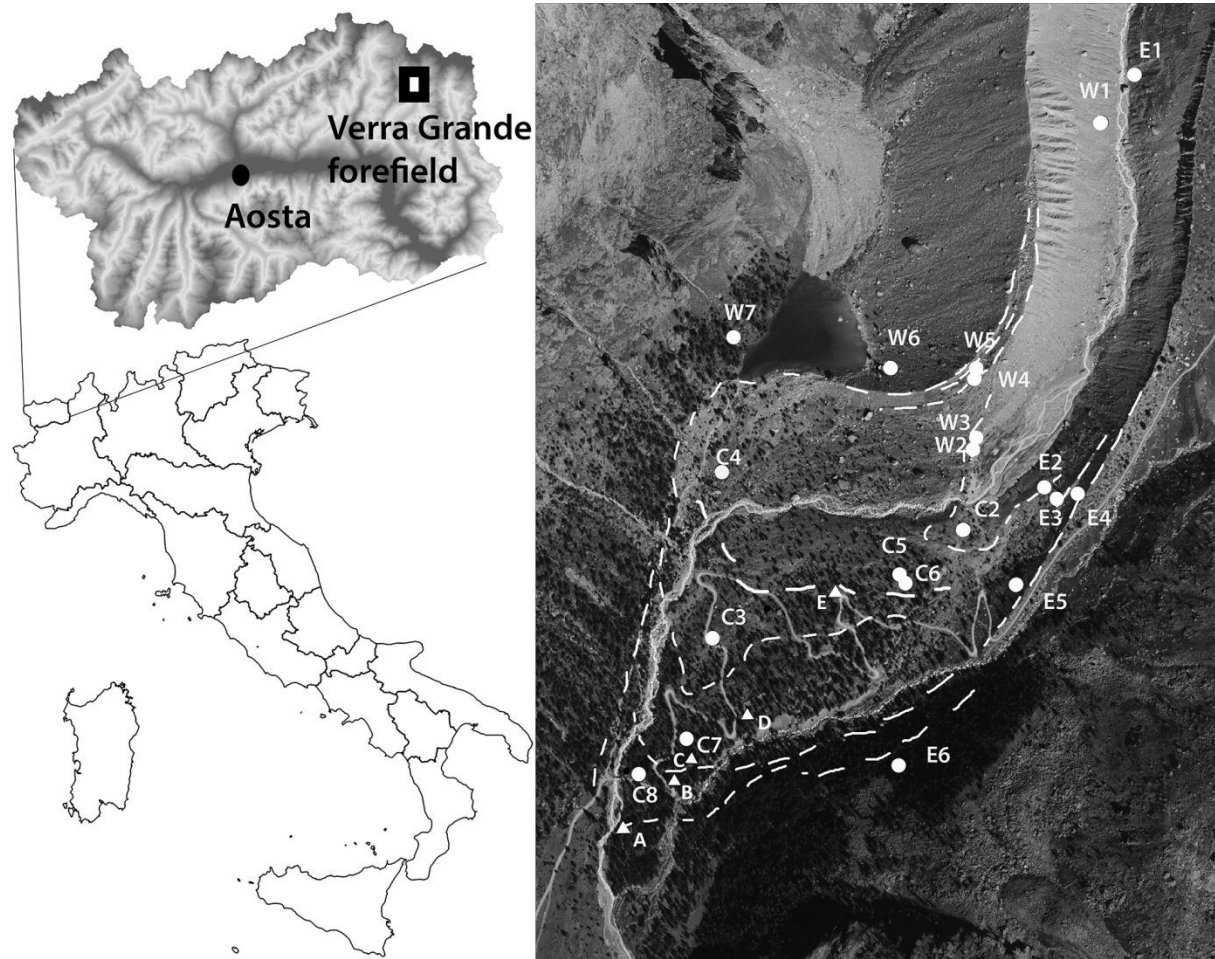


Fig. 2: X-ray diffraction patterns of the coarse sand fraction of C horizons from the eastern and western initial terms of the chronosequence parent. d-spaces are in Å. Abbreviations are as follows: SRP: serpentine minerals; QZ: quartz; AKF; alkali-feldspars; PLG: plagioclases.

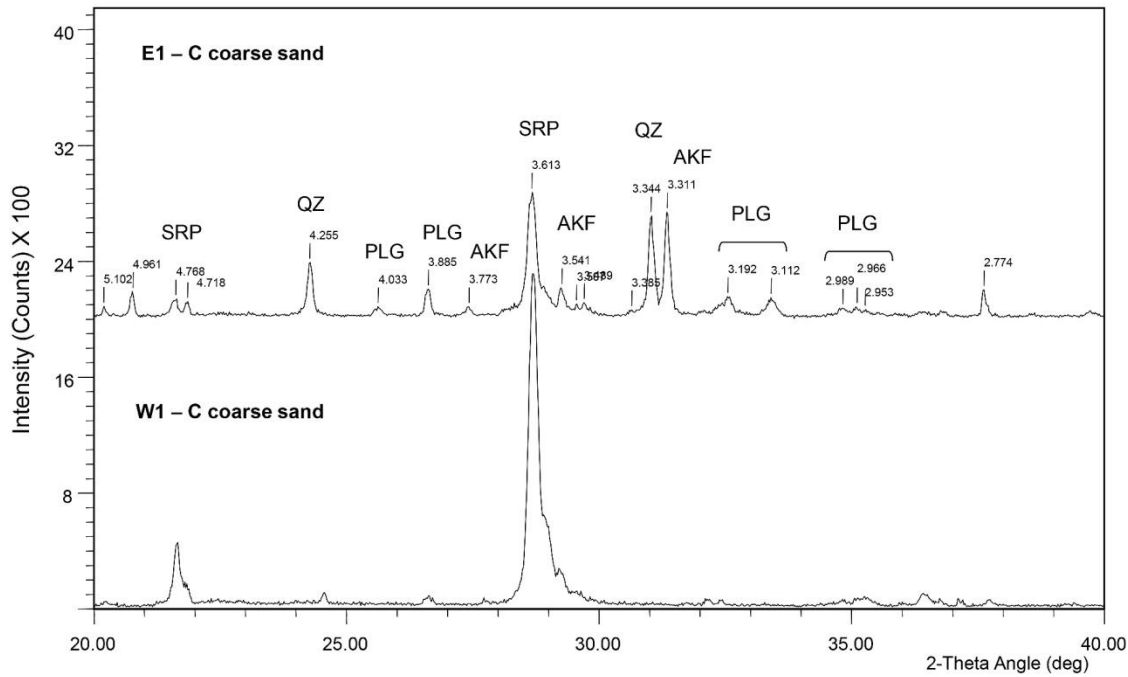
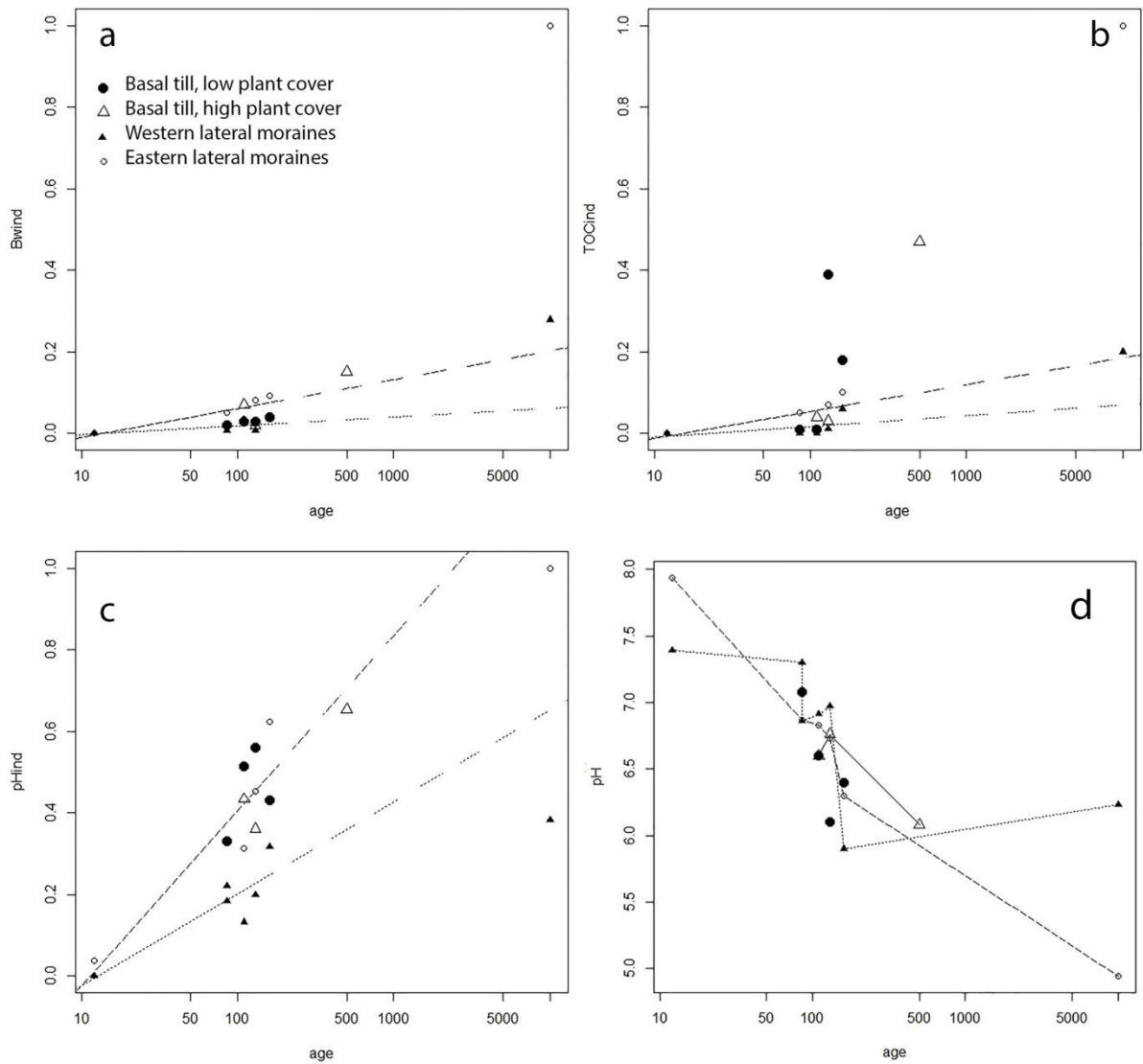


Fig. 3: Time trends of pedogenic development indicators: the Buntley and Westin color index (BWind, a); the TOC normalized by horizon and profile thickness (TOCind, b); the difference between pH values in soil horizons and the initial soil normalized by profile thickness (pHind, c); and the pH values. The dashed and the dotted lines in (a), (b) and (c) show the significant chronofunctions of the indicators respectively in eastern and western lateral moraines, calculated on LIA soils; the change in the line style denote the end of the validity range of the chronofunctions. Broken lines in (d) are drawn to better show trends



795 Fig. 4: Changes with age of deposition of the moraines of: N (%); Ca/Mg ratio (b); available P
796 (P_{olsen}) (c); exchangeable Ni (d); on the eastern lateral moraine system (empty circles, dashed
797 lines), on the western one (filled triangles, dotted lines), in forested flat basal till (large, empty
798 triangles, large dashed lines) and under pioneer vegetation on flat basal till (large filled
799 circles, solid lines). All values are derived from surface horizon analysis. The dashed and the
800 dotted lines in (b) and (c) show the significant chronofunctions of the considered properties
801 respectively in eastern and western lateral moraines, calculated on LIA soils; the change in the
802 line style denote the end of the validity range of the chronofunctions. Broken lines are drawn
803 to better show trends.

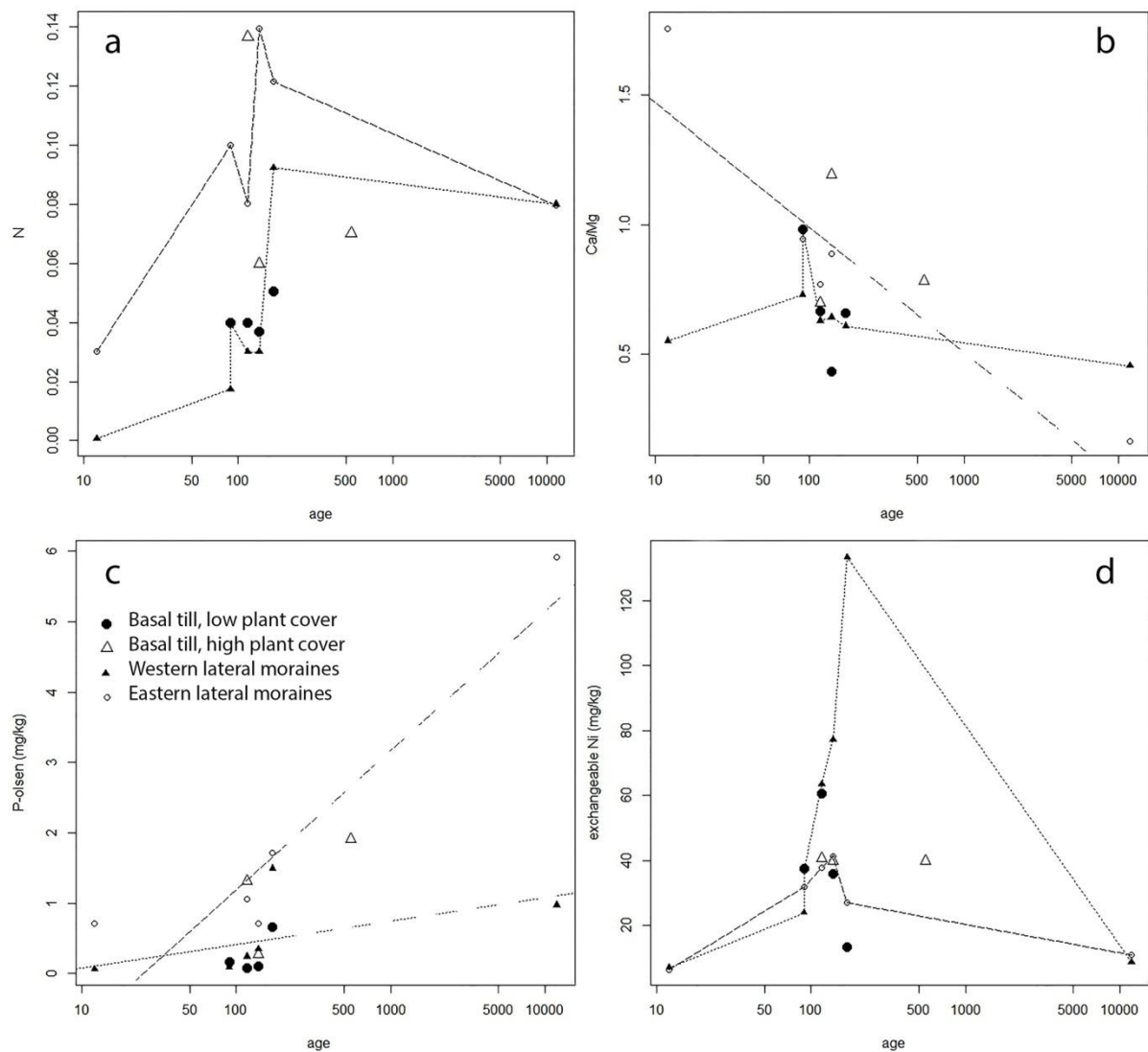
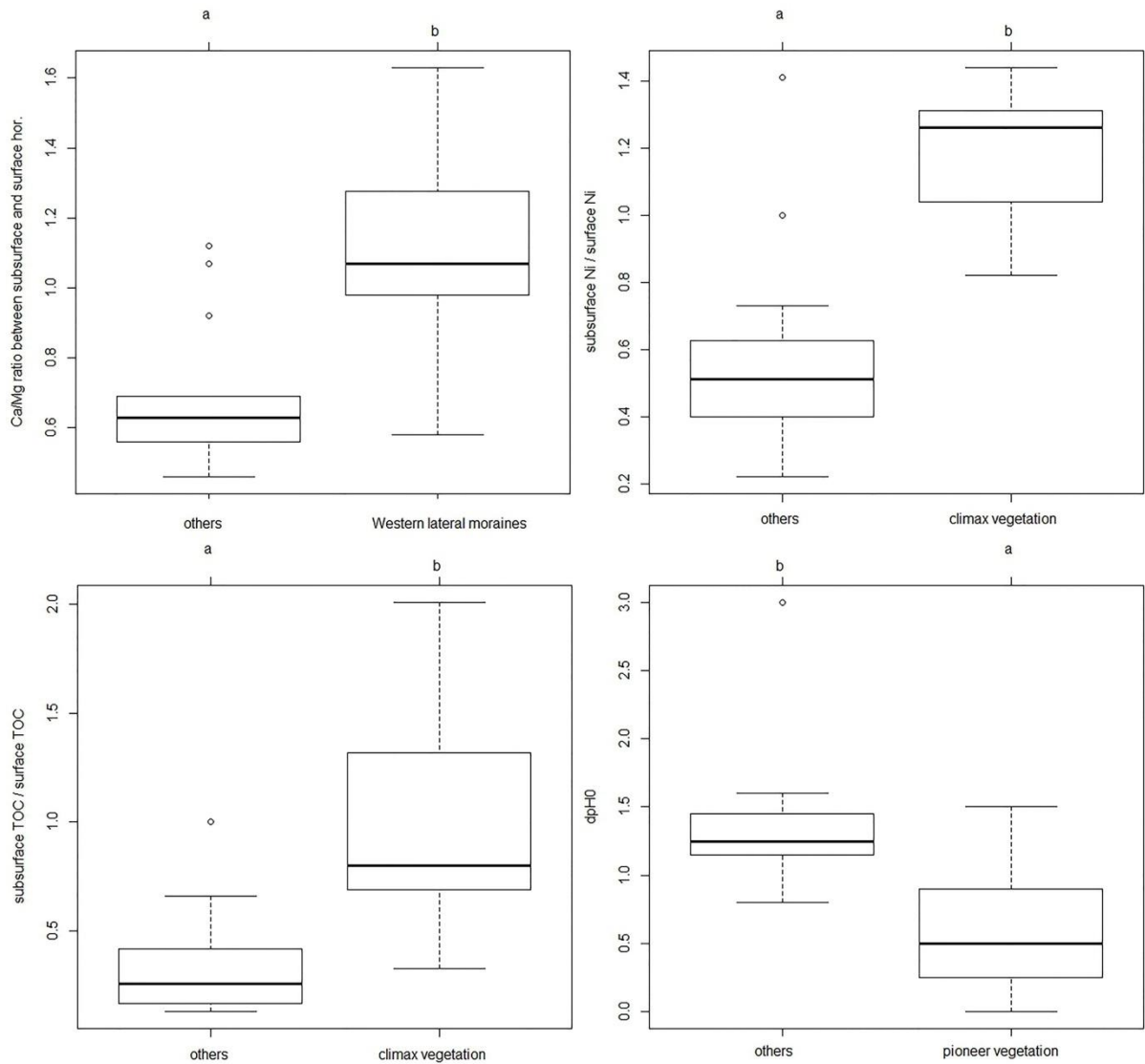


Fig. 5: Different Ca/Mg ratio in subsurface and surface horizons, indicated by the ratio between their respective values, in the western lateral moraines (a); ratio of exchangeable Ni (b) and TOC concentrations (c) in subsurface and surface horizons under climax or quasi-climax vegetation, the pH value decrease since moraine deposition, evidenced by the difference between the initial pH values and the value in each surface horizons, under pioneer plant communities or under other vegetation types (d). The dominance of ericaceous shrubs in the understory was used as indicator of climax plant communities. $p < 0.05$.



815 Fig. 6: Conceptual diagram of factors influencing the speed of soil formation processes in the
816 Verra Grande proglacial area.

	Steep lateral moraines		Flat basal till
Parent material	10% Gneiss		100% Serpentine
Initial soil conditions	Alkaline pH, Traces of CaCO ₃ , High Ca/Mg, Moderate available P, Low N, Low TOC, High exchangeable Ni		Subalkaline pH, Traces of CaCO ₃ , Low Ca/Mg, Very low available P, Low N, Low TOC, High exchangeable Ni
Plant encroachment	Fast	Slow	Slow / fast in later stages
Slope effect (erosion)	Initially strong, then moderate	Strong	Slow
Ericaceae / forest encroachment	Late (centuries)	Late (millennia?)	Early (patches), complete (few centuries)
			Forest / Ericaceae Pioneers
Cryoturbation	Initially strong, then moderate	Strong	Weak Strong
TOC accumulation	Moderate	Slow	Moderate Slow
Acidification	Moderate	Slow	Moderate Slow
P Biocycling	Moderate	Almost absent	Strong Almost absent
Ca Biocycling	Slow, then Ca leaching	Slow	Slow, then Ca leaching Slow
Ni availability	Slow increase, then leaching	Fast increase, then leaching	Slow increase, then leaching Moderate increase
Podzolization	Millennia	Not detected	Centuries Centuries (after substitution of pioneer vegetation)

817

818

819

Fig. 7: Soil formation rate according to the method described by Egli et al. (2014) and the TOC accumulation index (TOCind) in Verra Grande forefield (the eastern, western and central moraine systems are represented by respectively full circles, triangles and squares), in the Morteratsch forefield (number 4, from Egli et al. 2012 and Egli et al. 2014) and in the Lys forefield (number 5 for forest habitats and number 6 for subalpine grassland, from D'Amico et al. 2014a).

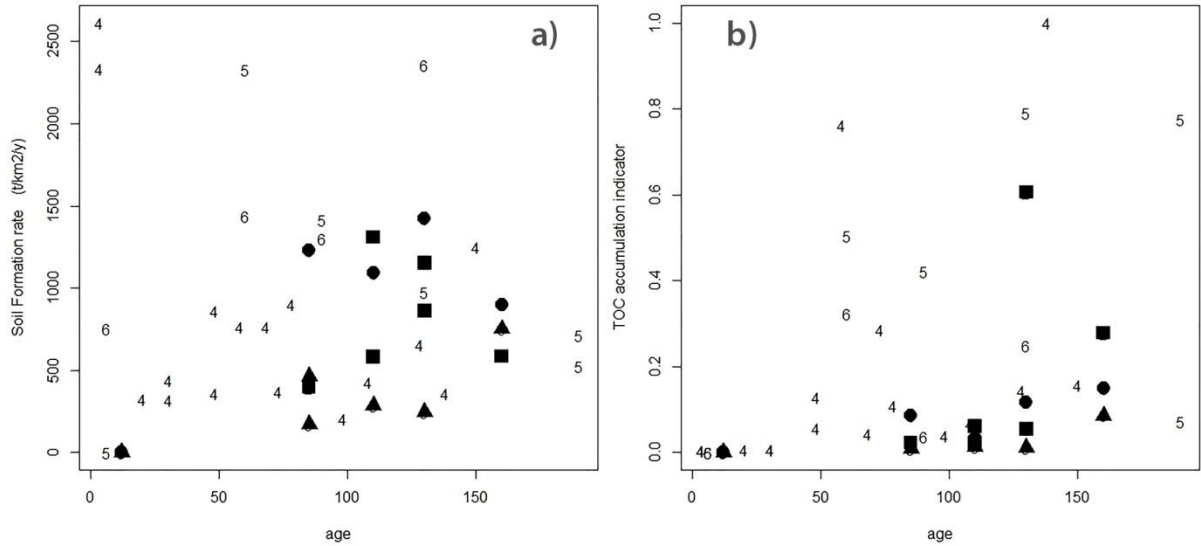


Table 1: main environmental properties of the study sites

site ^a	Year of deposition ^b	Elevation (m a.s.l.)	Aspect (°N)	Slope steepness (%)	bare soil (%)	Tree cover (%)	Parent material ^c
C2	1950	2255	200	1	40	30	SP
C3*	1880	2132	180	3	50	80	SP
C4	1921	2185	180	3	25	10	SP
C5	1921	2235	180	5	40	10	SP
C6*	1921	2235	180	8	20	20	SP
C7	1861	2120	180	3	40	60	SP
C8*	~1820-1300?	2080	160	10	0	80	SP
E1	2000	2318	270	35	50	0	SP (10% GN)
E2	1950	2260	250	25	20	5	SP (10% GN)
E3	1921	2275	260	35	30	5	SP (10% GN)
E4	1861	2285	260	30	1	5	SP (10% GN)
E5	1821	2250	300	30	0	5	SP (10% GN)
E6*	LG	2200	300	30	0	60	SP (<5% GN)

W1	2000	2315	90	35	99	0	SP
W2	1950	2252	60	10	85	0	SP
W3	1950	2257	60	30	40	30	SP
W4	1921	2260	240	30	75	0	SP
W5	1861	2265	240	30	50	0	SP
W6	1821	2225	300	35	20	1	SP
W7*	LG	2230	110	30	0	60	SP

830

831 ^a: high ericaceous cover in the understory is evidenced by the * next to the site symbol

832 ^b: LG: Late Glacial, around 11500 years BP

833 ^b: SP: serpentinite, GN: gneiss

834

835 Table 2: selected macromorphological properties of the soils along the Verra Grande
836 chronosequence. Oi horizons, 0.5 to 3 cm thick, were omitted from the list.

Site	Horizon	Depth (cm)	Color (Munsell, dry)	Structure ^a	Roots ^b	Rock fragments ^c (%)	Silt caps ^d
W1	C	0-25+	Gley1-6/10Y	AB	A	60	1
W2	A	0.5-3	5Y 5/2	GR, 2, w	A	30	
	C	3-21	5Y 5/1	L, 2, w	C	60	
	2C	21-35+	Gley1-6/10Y	L, 4, s	A	10	1
W3	AC	0-7	5Y 5/2	GR, 2, w	S	70	
	C	7-20+	Gley1-6/10Y	L, s, m		70	1
W4	O (biotic crust)	discontinuous					
	A	0-3	5Y 4/2	GR, 2, w	A	30	
	AC	3-10	5Y 5/2	GR, 2, w			
	C1	10-17	5Y 5/1	GR, 2, w	S	60	1
	C2	17-30+	Gley1-5/10Y	L, 4, w	A	60	1
W5	O (biotic crust)	0-0.4	2.5Y 2/1				
	A	0.4-4	5Y 5/1	GR, 2, w	AA	50	
	C1	4-17	Gley1-6/10Y	GR, 1, w	S	60	1
	C2	17-30+	Gley1/G	VS		70	2
W6	O (biotic crust)	0-0.2	2.5Y 2/1				
	A	0.2-8	2.5Y 2.5/1	GR, 2, w	AA	50	
	CA	8-19	5Y 4/1	GR, 2, w	A	70	
	C	19-40+	5Y 5.5/1	VS	S	80	2
W7	Oe/Oa	2-3					
	A	3-10	2.5Y 3.5/3	GR, 1, w	AA	10, WW	
	Bw	10-24	2.5Y 5.5/6	SP, w, fi	A	60	
	C	24-35+	2.5Y 5/3	SP, s, m	C	60	
E1	C1	0-8	5Y 5/1	AB	C	50	
	C2	8-30+	Gley1-6/10Y	AB	S	50	1
E2	Oe	0-1	10YR 2/1		A	0	
	A	1-9	5Y 4/3	GR, 1, w	A	30	
	AC	9-20	5Y 4/1	AB	A	60	
	C	20-40+	Gley1-4/10Y	AB	S	50	2
E3	A	0-3	5Y 3/2	GR, 1, w	A	50	
	CA	3-23	5Y 4/1	GR, 1, w	C, m	50	
	C	23-40+	Gley1-5/10Y	VS	S	60	2
E4	Oe	0-2	10YR 2/1	GR, 2, w	A		
	A	2-12	5Y 4/2 (60%), 2.5Y 3/2 (40%)	GR, 2, w	A	50	
	CA	12-30	5Y5/2	GR-SP, 2, w	C, m	60	2
	C	30-40+	Gley1-5/10Y	VS	S	90	3
E5	Oa	1-2	10YR 2/1	M	AA		
	AC	2-13	2.5Y 5/3	SP, 2, m	C, m	60	2

E6	C	13-50+	5Y 5/1	VS, s	C	70	3
	Oe	2-5					
	Oa	5-12	7.5YR 2/1	M			
	E	12-21	10YR 6/2	L, 4, w	C	10 WW	
	Bs1	21-42	7.5YR 5/4	SP, 3, m	C, co	20 WW	
	Bs2	42-63+	7.5YR 5/4	SP, 3, m	S, C, co	50 W	
C2	A	0.5-7	5Y 5/2	GR, 2, w	A	30	
	C	7-30+	5Y 5/1	L, 2, w	C	60	1
C3	Oe	4-7			A		
	A	7-10	5Y 4/2	GR, 2, w	A	50	
	AB	10-18	2.5Y 5/3	SP, 2, m	C	50	
	C	18-30+	Gley1-5/10Y	VS	S	70	2
	Oe	0-2	10YR 2/1	GR			
	A	2-8	2.5Y 4/2	GR, 2, w	C	50	
C4	C1	8-21	5Y 5/1	L, 2, w	C	50	2
	C2	21-35	5Y 5/1	VS	S	60	3
C5	Oe	0.5-3					
	A	3-7	Gley1 4/1	GR, 2, w	C	50	
	CA	7-21	5Y 5/1	GR, 2, w	C	60	
	C	21-32+	Gley1 5/5GY	VS	S	60	1
C6	Oe	1-4		M			
	A	4-9	2.5Y 2.5/1	GR, 2, w	C	40	
	AC	9-25	5Y 4/1	GR, 2, w	S	60	
	C	25-34+	5Y 5/1	VS	S	70	
C7	Oe	1-2					
	Oa	2-4			AA		
	A1	4-8	5Y 4/2 (2.5Y 3/2, 30%)	GR, 2, w	A	30	
	AC	8-18	5Y 5/2	GR, 2, w	C, m	60	1
	C	18-23+	Gley1-5/10Y	VS, cemented	S	60	3
C8	Oe-Oa	3-9	7.5YR 2/1	M	A		
	E	9-13	2.5Y 5/2	L, 3, w	A, m	20, WW	
	Bs	13-21	10YR 4/3	GR, 3, w	C	50, W	
	C	21-50+	5Y 5/1	VS	S	60	3

837

838 ^a GR: granular; PL: platy; PS: subangular blocky; MA: massive; RS: rock structure; AB:
839 absent; M: matted (O horizons). 1: very fine; 2: fine; 3: medium; 4: coarse. W: weak; m:
840 moderate; s: strong.

841 ^b AA: very abundant; A: abundant; C: common; S: scarce. m: mid-sized roots; co: coarse
842 roots.

843 ^cW: weathered; WW: highly weathered

844 ^d1: silt caps up to 1 mm thick, visible on few rock fragments; 2: silt caps up to 2 mm thick,

845 visible on many rock fragments; 3: silt caps up to 2 mm thick, visible on most rock fragments

846 Table 3: Ammonium oxalate- (Fe_{ox} , Al_{ox}) and dithionite-citrate-bicarbonate (Fe_d , Al_d)
847 extractable Fe and Al in the oldest soils from the Western, Eastern and Central parts of the
848 study area.

		$\text{Fe}_{\text{ox}}(\text{g kg}^{-1})$	$\text{Al}_{\text{ox}}(\text{g kg}^{-1})$	$\text{Fe}_d(\text{g kg}^{-1})$	$0.5\text{Fe}_{\text{ox}}+\text{Al}_{\text{ox}}$ (%)
W7	A	1.90	0.30	12.93	0.12
	Bw	1.53	0.27	13.40	0.10
	BC	1.02	0.28	7.52	0.08
E6	E	4.66	1.48	9.84	0.38
	Bs1	10.07	2.86	20.10	0.79
	Bs2	11.25	3.21	21.25	0.88
C8	E	3.85	0.25	4.70	0.22
	Bs	6.85	0.35	11.60	0.37
	C	4.23	0.20	3.15	0.23

849

850

851 Table 4: Chemical properties of the soils along the Verra Grande chronosequence. When a
852 cell is empty the property was not determined.

Profile	Horizon	pH	CaCO ₃ g kg ⁻¹	C g kg ⁻¹	C/N	Mg cmol _c kg ⁻¹	Ca/Mg	Ni _{ex} mg kg ⁻¹	P _{olsen} mg kg ⁻¹
W1	C	7.4	4.0	5.0		0.39	0.55	6.99	0.06
W2	A	6.9	0.0	6.1	15.3	0.66	0.73	23.88	0.17
	C	7.5	0.0	1.0		0.41	0.88	12.21	
	2C	7.6	1.2	0.1					
W3	AC	7.3	0.0	2.6	8.7	1.17	0.98	37.37	0.09
	C	7.8	0.0	1.5		4.35	0.06	24.12	
W4	O (bioticcrust)	7.0		19.3	14.9	1.74	0.89	76.43	
	A	6.9	0.0	3.5	11.7	0.74	0.63	63.42	0.24
	AC	7.1	0.0	2.3	11.1	0.32	1.03	46.02	
	C1	7.4	2.0	1.2	9.8	0.25	1.12	19.21	
	C2	7.5	3.2	0.2		0.38	1.16	18.99	
W5	O (bioticcrust)	6.5		16.8	14	2.07	0.66	4.62	
	A	6.9	0.0	4.0	13.3	0.97	0.64	77.16	0.35
	C1	7.6	1.1	1.0		0.36	0.86	39.41	
	C2	7.5	0.9	bdl		0.24	1.09	13.79	
W6	O (bioticcrust)	5.9		32.1	15.1				
	A	5.9		13.2	14.3	2.62	0.61	133.43	1.50
	CA	7.0	4.0	5.4	15.1	1.21	0.65	62.21	
	C	7.1	2.1	0.6		0.44	0.97	40.82	
W7	Oe/Oa	5.6		296.0	23.7				
	A	6.2		18.2	21.5	3.93	0.45	8.70	0.98
	Bw	6.3		12.6	21	3.59	0.43	9.02	
	C	6.4		3.0	15	1.99	0.40	2.63	
E1	C1	7.9	1.0	4.0	12.9	0.39	1.75	6.41	0.72
	C2	8.0	5.0	0.5		1.68	1.08	3.16	
E2	A	6.9	0.0	19.5	19.5	0.92	0.95	31.94	0.12
	AC	7.8	1.0	5.1	12.8	0.88	1.06	19.22	
	C	7.8	1.0	0.2		1.25	0.43	4.61	
E3	A	6.8	0.0	11.3	14.1	2.11	0.77	37.72	1.06
	CA	7.2	0.0	1.7	8.5	1.50	0.39	11.54	
	C	7.6	0.0	0.2	20	1.38	0.40	6.28	
E4	A	6.7	0.0	17.3	12.4	1.97	0.89	41.33	0.71
	CA	6.8	0.0	3.1	10.3	1.89	0.41	9.18	
	C	6.7	0.0	1.4		1.08	0.44	8.51	
E5	Oa	6.3		86.6	12.7				
	AC	6.3	4.0	18.6	14.1	2.59	0.66	26.95	1.71
	C	7.1	4.0	2.8	9.3	1.55	0.61	13.23	
E6	Oe	4.8		295.4	24.6				
	Oa	4.6		175.0	22.2				
	E	4.9		22.1	28.5	6.27	0.16	10.77	5.92

	Bs1	5.4		17.7	18.9	5.15	0.10	14.11	
	Bs2	5.6		17.7	16.2	4.99	0.11	16.94	
C2	A	7.1	0.0	6.7	16.5	1.17	0.98	37.33	0.17
	C	7.6	3.0	2.1	19.2	0.68	0.66	19.00	
C3	A	6.6	0.0	21.1	24.4	4.65	0.70	40.73	0.1
	AB	6.9	0.0	7.0	17.5	1.41	0.46	33.49	
	C	7.0	0.0	2.3	23	1.26	0.44	63.31	
C4	A	6.6	3.0	7.0	17.4	1.43	0.67	60.71	0.27
	C1	7.6	2.0	3.0	14.9	1.96	0.38	17.64	
	C2	7.7	6.0	1.1		1.61	0.29	3.36	
C5	Oe	6.5		281.0	23.93				
	A	6.7	0.0	11.4	19.0	1.66	0.70	39.86	0.09
	CA	7.2	1.0	4.3	20.6	1.01	0.48	56.29	
	C	7.3	2.0	2.4	15.3	1.13	0.42	39.11	
C6	Oe	5.9		305.5	26.1				
	A	6.1	0.0	7.3	24.4	1.38	0.43	35.86	1.31
	AC	6.7	0.0	14.7	22.8	3.00	0.46	51.58	
	C	7.0	0.0	3.4	18.64	2.21	0.44	48.21	
C7	Oa	6.3		241.1	25.1				
	A1	6.4	0.0	10.1	20.0	2.35	0.66	13.35	0.66
	AC	7.1	0.0	2.3	11.5	1.38	0.37	5.22	
	C	7.1	0.0	1.1		1.21	0.34	1.89	
C8	Oe-Oa	5.8		210.5	19.5				
	E	6.1		11.7	16.7	1.03	0.78	39.86	1.91
	Bs	6.6	0.0	15.4	17.1	3.71	0.37	50.10	
	C	7.1	0.0	2.5	12.5	2.16	0.34	30.84	

853

854 Bdl: below instrumental detection limit

855

856 Table 5: Pearson's correlation coefficient among chemical and site properties in the Verra
857 Grande soil chronosequence

	pH	Ca _{ex}	Mg _{ex}	K _{ex}	Ca _{ex} /Mg _{ex}	Ni _{ex}	TOC	C/N	P _{Olsen}	age	slope	asp	tcov	NS	NIBA
Ca _{ex}	-0.11	1													
Mg _{ex}	<u>-0.72</u>	<u>0.57</u>	1												
K _{ex}	-0.24	<u>0.88</u>	<u>0.53</u>	1											
Ca _{ex} /Mg _{ex}	<u>0.71</u>	0.24	<u>-0.47</u>	0.21	1										
Ni _{ex}	-0.17	0.00	-0.12	0.12	-0.11	1									
TOC	<u>-0.53</u>	<u>0.73</u>	<u>0.78</u>	<u>0.61</u>	-0.23	-0.04	1								
C/N	<u>-0.62</u>	0.33	<u>0.77</u>	0.34	-0.43	-0.35	<u>0.65</u>	1							
P _{Olsen}	<u>-0.75</u>	0.16	<u>0.8</u>	0.22	-0.42	-0.12	<u>0.52</u>	<u>0.58</u>	1						
Age	<u>-0.58</u>	0.07	<u>0.72</u>	0.05	<u>-0.48</u>	-0.33	0.36	<u>0.63</u>	<u>0.67</u>	1					
Tree cover	<u>-0.52</u>	0.38	<u>0.59</u>	<u>0.5</u>	-0.3	-0.29	<u>0.54</u>	<u>0.72</u>	<u>0.46</u>	<u>0.46</u>	-0.41	-0.22	1		
Bare soil	<u>0.68</u>	-0.32	<u>-0.49</u>	-0.36	0.17	-0.06	<u>-0.56</u>	-0.33	<u>-0.49</u>	-0.42	-0.04	<u>-0.44</u>	-0.36	1	
NIBA	-0.43	-0.11	0.25	-0.10	-0.3	-0.24	0.13	<u>0.53</u>	0.32	0.41	-0.19	-0.24	0.42	-0.11	1
pHBA	-0.26	-0.19	0.01	-0.19	-0.21	-0.10	0.09	0.32	0.07	-0.06	<u>-0.47</u>	0.04	0.10	-0.25	-0.01
camgBA	0.14	<u>-0.48</u>	-0.28	<u>-0.54</u>	-0.28	0.31	-0.3	-0.26	-0.27	-0.05	0.25	0.00	<u>-0.45</u>	0.43	0.07
Ericaceae	<u>-0.68</u>	-0.10	<u>0.49</u>	0.04	<u>-0.45</u>	-0.26	0.27	<u>0.54</u>	<u>0.66</u>	<u>0.75</u>	0.01	-0.03	<u>0.65</u>	<u>-0.55</u>	<u>0.64</u>

858

859